DYNAMICAL ANALYSIS OF HUMAN WALKING

Marek Wojtyra
Institute of Aeronautics and Applied Mechanics
Warsaw University of Technology,
Nowowiejska 24, 00-665 Warsaw, POLAND
E-mail: mwojtyra@meil.pw.edu.pl

1. Introduction

Researches into human gait have a wide range of applications in medicine, ergonomics, sport science and technology. Most often methods of multibody dynamics are used when investigation is focused on mechanical aspects of the gait (Allard et al., 1995; Berme & Cappozzo, 1990; Winter, 1979; Vaughan, 1992).

The inverse dynamics approach is commonly adopted in a human gait analysis. Displacements of the human body segments and ground reaction forces are known from measurements. The joint reaction forces and muscle net torques (which cannot be measured directly) are calculated. Since the ground reaction forces are known it is not necessary to model the foot-ground contact. The inverse dynamics approach requires measured displacements to be differentiated twice in order to obtain accelerations. The choice of filtering and smoothening methods affects significantly the obtained results (Allard et al., 1995, Vint & Hinrichs, 1996). The errors in alignment of ground reaction force and foot affect the results as well (McCaw & DeVita, 1995).

In this paper a direct dynamics approach to the human gait analysis is presented. The direct dynamics approach is usually taken when a walking machine with its control system is investigated. It is seldom used to human gait simulation.

In the presented model the measurements of displacements of the human body segments are treated as a gait patterns (i.e. the patterns of relative motion in joints). The net torques (generated in the way that enables realisation of the gait patterns) are applied to a mechanical system and the direct problem of dynamics is solved. The foot-ground contact is modelled. For the gait stabilisation a simple closed loop control algorithm is introduced into the simulational model.

The non-trivial problems: transforming measured displacements into gait patterns, building a model of the foot-ground contact and introducing a proper control algorithm are discussed in the paper.

Though the method presented here is more complicated than the traditional one, there are some advantages. It is possible to predict system behaviour, whereas inverse dynamics approach is restrained to reconstruction only. Moreover, since accelerations are calculated, there is no need to differentiate measured displacements twice. Ground reaction forces as well as feet positions are calculated, so the alignment of foot position with reaction force is no longer a problem. And finally, the simulation is not limited by the number of measured gait cycles (usually one or two), since gait patterns can be extrapolated.

2. Multibody model

2.1. Background

There exist various methods for modelling bipedal walking. Some multibody models for the gait simulation represent bipeds of a very simple (not anthropomorphic) kinematic structure (e.g. the three-body-model - Bourassa et al., 1997). Other models are limited to two dimensions (Pandy & Berme, 1988; Koopman et al., 1995; Ouezdou et al., 1998, Wojtyra 1998).

Walking is a special kind of the multibody system motion with the occurrence of impacts, friction and slipping. All these phenomena observed during the foot-ground contact have to be introduced into the model to make it realistic. In some multibody models of the biped the foot-ground contact is modelled by the additional kinematic joint (Onyshko & Winter, 1980; Pandy & Berme, 1988) or temporal fixing of the supporting foot to the ground (Blajer & Schiehlen, 1993). Different models are used for single and double support phases. In this type of models the non-slip and non-impact conditions are assumed.

There is another group of models, in which the forces between foot and ground are modelled in a more realistic way (Gerristen et al., 1995; Gilchrist & Winter, 1996; Güler et al., 1998; Wojtyra, 1998, 1999). Control of the model of this type is more difficult, since the control system must prevent the biped from slipping and the biped must absorb the shocks caused by impacts.

The model presented here is three-dimensional and reflects the kinematic structure and mass properties of the human locomotion apparatus. Both the slips and impacts are taken into consideration. The model was prepared and investigated in ADAMS environment.

2.2. Kinematical and mass properties

The model and its kinematic scheme is presented in the Fig. 1. The model consists of 8 rigid parts (plus 8 additional, massless bodies). For the sake of simplicity, the trunk is modelled as two parts connected by revolute joint. The inertia properties of head and arms are included in trunk properties. Lower parts of human body are modelled more realistically. Each leg consists of 3 parts: thigh, shank and foot. Each hip joint is modelled as three consecutive revolute joints. Massless bodies are used to establish connection between joints (the connection between trunk and thigh is modelled as follows: trunk - joint 1 - massless body 1 - joint 2- massless body 2 - joint 3- thigh). These three joints are kinematically equivalent to a spherical joint. Three

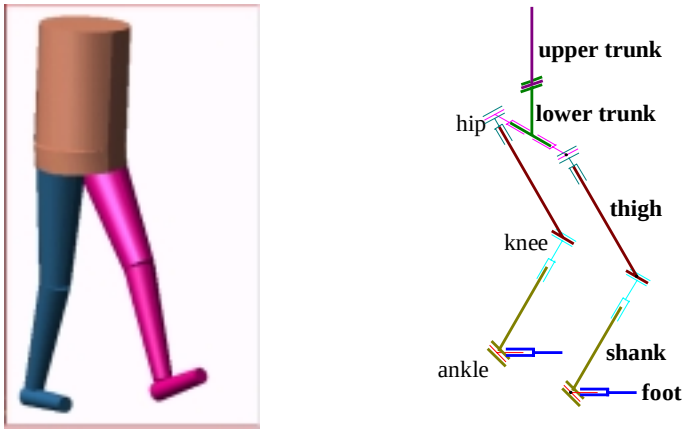

Figure 1. The model general view and kinematic scheme.

revolute joints were applied in order to enable an imposition of motion constraints. Each knee joint is modelled as two consecutive revolute joints and one massless body. Each ankle joint is modelled as two consecutive revolute joints and one massless body. The modelled biped has 21 degrees of freedom. Each revolute joint is additionally constrained by a motion generator, but motions are active only at the start of simulation to set appropriate initial position of the model.

The dimensions and mass properties of the parts are based on available statistical data (Seireg & Arvikar, 1989) and are parametrised. This feature of the model enables investigation of different subjects. The body segments are modelled as frustums with homogenous mass distribution. The table 1 shows dimensions and mass properties of an average male.

Table 1. Geometrical and mass properties of the average male.

Height [m]		1.75				
Body mass [kg]		72				
Distance between hips [m]		0.18				
Part name		Upper trunk	Lower trunk	Thigh	Shank	Foot
Frustum length [m]		0.44	0.088	0.435	0.425	0.25
Bigger frustum diameter [m]		0.336	0.336	0.18	0.116	0.072
Smaller frustum diameter[m]		0.336	0.336	0.116	0.072	0.06
Density [kg/m^3]		1020	1020	980	1200	1300
Mass [kg]		39.8	7.96	7.45	3.60	1.11
CM moments of inertia	*I_{zz} [kgm^2]* **	0.561	0.112	$2.19 \cdot 10^{-2}$	$4.34 \cdot 10^{-3}$	$6.15 \cdot 10^{-4}$
	$I_{xx} = I_{yy}$ [kgm^2]	0.923	$6.01 \cdot 10^{-2}$	0.123	$5.34 \cdot 10^{-2}$	$6.06 \cdot 10^{-3}$

2.3. Ground reaction forces

The impact and friction effects are considered in the ground reaction forces modelling. The ground is represented by a flat rigid surface. A set of 5 three-component force vectors acting on each foot is used to model ground reaction forces. The pressure and the shape of contact area between human foot and ground changes during walking. In the model the number of forces and points of their applications (*I-marker* positions) were chosen to adequately reproduce the reality. The distribution of three-component force objects acting on a foot is shown in the Fig. 2.

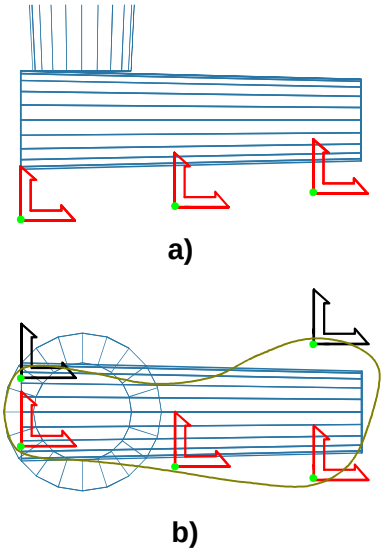

Figure 2. Ground reaction forces acting on foot.
a) side view, b) top view.

Normal to the ground (ground surface coincides with xy plane of global coordinate system) reaction force F_z is modelled using *IMPACT* function:

$$F_z = \begin{cases} \mathrm{MAX}(0\ ,\ -k\,d_z - c\,v_z) & d_z < 0 \\ 0 & d_z \geq 0 \end{cases}$$

where:

d_z - *z* coordinate of three-component force *I-marker*,
v_z - *z* component of velocity ($v_z = \dot{d}_z$),
k - stiffness,
c - damping.

Damping c is a non-linear function of ground penetration p_z (p_z = MAX[0, $-d_z$]):

$$c = \begin{cases} c_{max} \left| \frac{3}{h^2} p_z^{\,2} - \frac{2}{h^3} p_z^{\,3} \right| & p_z < h \\ c_{max} & p_z \geq h \end{cases}$$

where:

h, c_{max} - constant values.

A number of test simulations was performed in order to choose proper values of estimated stiffness *k* of the foot in shoe and proper values of damping parameters *h* and c_{max}. The ground penetration p_z corresponds to the deflection of foot and shoe during walking. The maximum value of p_z observed during simulation was equal to 2 cm, which agrees well with experimental data (Güler et al., 1998). The chosen level of damping is high enough to prevent the foot from "jumping" after hitting the ground, which also agrees with experiments. The choice of parameters *k*, c_{max} and *h* is not crucial - it was proved that after the 20% change of the value the model behaviour has remained almost unchanged. The chosen values are: $k = 1.5 \cdot 10^4$ N/m, c_{max} = 1500 Ns/m, *h* = 0.01 m.

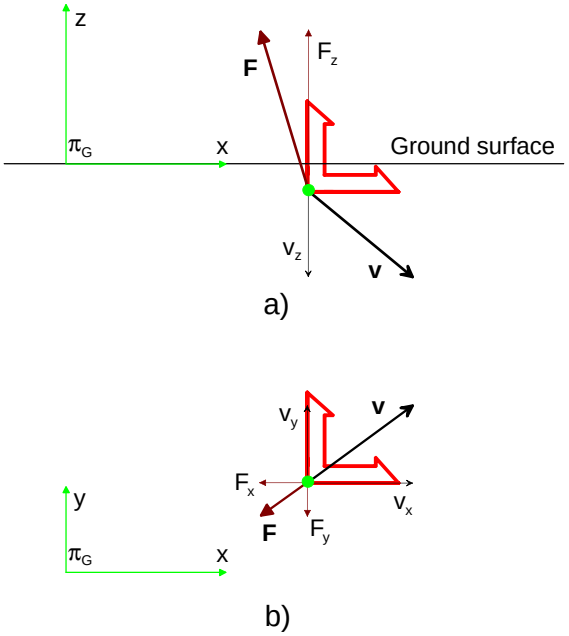

Figure 3. Three-component force object - force and velocity: a) side view, b) top view.

The tangent reaction force *T* is represented in terms of a pseudo-Coulomb friction model (in this model of friction there is no stiction, i.e. the bodies are moving relative each other at a negligibly small velocity). At the beginning velocity of sliding is calculated:

$$v_p = \sqrt{v_x^{\,2} + v_y^{\,2}}$$

where:

v_x - *x* component of velocity of three-component force *I-marker*,

v_y - *y* component of velocity of three-component force *I-marker*.

Then a modulus of friction force is calculated:

$$T = \mu' \, F_z$$

where:

μ' - non-constant friction coefficient.

The dependence of μ' on v_p is given by the following formula:

$$\mu' = \mu \, \frac{2}{\pi} \operatorname{arctg} \frac{v_p}{\lambda}$$

where:

μ - Coulomb friction coefficient (constant value),

λ - constant value.

Finally, the tangent force components are calculated:

$$F_x = -T\frac{v_x}{v_p + \varepsilon}, \quad F_y = -T\frac{v_y}{v_p + \varepsilon}$$

where:

ε - small constant value.

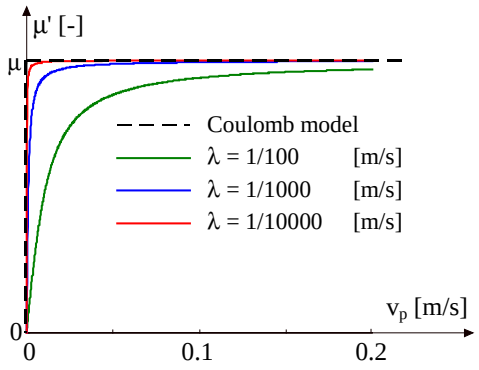

Figure 4. Friction coefficient dependency on the relative velocity.

The parameter λ has no physical meaning and is used only for numerical reasons. The typical Coulomb friction model introduces some discontinuities into the model, because it consists of two separate models for the stiction phase and for the sliding phase. The discontinuities are responsible for difficulties with the convergence of numerical integration of the differential-algebraic equations that describe the multibody system. The pseudo-Coulomb friction model is an approximation of the Coulomb model: instead of stiction phase, sliding with small velocity is observed. Both models are equivalent when the parameter λ tends to infinity, however if we choose a too small value of the parameter numerically stiff equations will result. For a relative velocity high enough the magnitude of T approaches the value $-\mu F_z$ given by the typical Coulomb friction model. Parameter ε was added in order to avoid division by zero when v_p tends to zero. After a number of test simulations following values were chosen: $\mu = 0.45$, $\lambda = 5 \cdot 10^{-4}$ m/s, $\varepsilon = 1 \cdot 10^{-8}$ m/s.

When $\mu' = 0.99\,\mu$ the observed sliding velocity is equal to 0.032 m/s which is negligibly small in comparison with average walking velocity equal to 1.4 m/s. It has been found that the multibody model behaviour sensitivity to the parameters λ and ε is low.

3. Control system

3.1. Gait patterns

Parameters characterising walk of the subject person were measured. A two-camera system was used to cinematographically measure trajectories of selected points of human body. The relative angles in each joint were calculated from the measurement results. The linear and angular parameters of absolute motion of the lower trunk were also calculated. The measured results were discrete. For the simulation purposes, however, a continuous and periodical function (periodical function can be easily extrapolated) is needed, which was obtained by approximating data by the appropriate Fourier series. These functions are called ‘gait patterns’. During approximation process periodicity and symmetry of the gait were assumed.

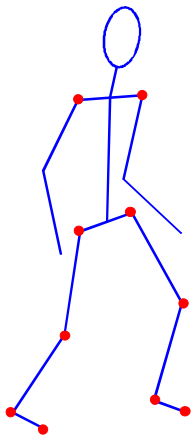

Figure 5. Selected points of human body.

It should be emphasised that measured functions are neither periodical nor symmetric. The difference between measured function and gait pattern is at some points bigger than measurement inaccuracy, which was shown in the Fig. 6.

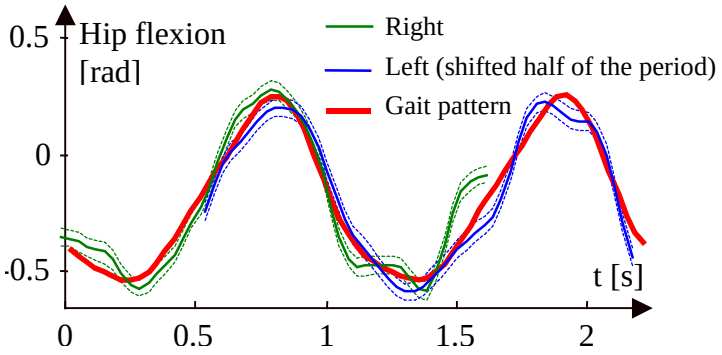

Figure 6. Differences between gait pattern and measurements results.

3.2. Driving torques

For the direct dynamics simulation all joints were equipped with actuators. The torque *M* generated by the actuator located in a joint was a function of: the current value of the joint angle φ, the "desired joint angle value" φ_0 given by the gait pattern and their time derivatives:

$$M = \kappa(\varphi_0 - \varphi) + \upsilon(\dot{\varphi}_0 - \dot{\varphi})$$

where:

κ, υ - constants.

This formulation of the torque equation (proposed earlier by Van den Bogert et al., 1989) ensures that the realised relative angle is close to the angle given by the gait pattern. The actuator can be treated as a motion generator (that strictly realises the gait pattern) connected in series with a spring-damper element. This spring-damper element is necessary to obtain a proper response to impacts (the system reaction to the impact is incorporated in the gait pattern, however heel strike occurs usually not exactly at the moment prescribed by the gait pattern - the system responses to the impact too early or too late).

Motion generators in joints were not used because as it was shown using a simpler (two-dimensional) model (Wojtyra, 1998) the exact reproduction of the gait patterns for joints leads to the biped fall. Due to both the measurement inaccuracy and additional operations (making it symmetric and periodical) the gait pattern suffers from relatively big errors. When gait patterns for joints are precisely realised the absolute motion of the trunk is left uncontrolled. If the biped started to fall the control system would not react. The only way to control the absolute motion of the trunk is to apply a control algorithm, which instantaneously modifies the prescribed joint motions in order to prevent the biped from loosing its stability.

3.3. Control algorithms

When the torques applied in joints depended only on current and desired value of the joint angle the relative positions of biped links with respect to each other were controlled, but the position of the whole biped with respect to the ground was not controlled. Therefore an additional external force and torque which supports the trunk was introduced. Each component *S* of the supporting force/torque was a function of: the current value of the linear/angular displacement ζ, the "desired value" ζ_0 given by the gait pattern for the trunk and their time derivatives:

$$S = \psi(\zeta_0 - \zeta) + \eta(\dot{\zeta}_0 - \dot{\zeta})$$

where: ψ, η - constants.

The values of the supporting force and torque can be recognised as the measure of the model and the gait patterns inaccuracies.

The concept of external force was helpful in the process of control algorithm synthesis. The proposed control algorithm is a heuristic one. It consists in incorporating some feedback information, i.e. some quantities dependent on the current position and orientation of the biped trunk (with respect to the ground) into the function defining the torques in selected joints.

The method for the control algorithm construction will be detailed considering a simple algorithm for the trunk yaw angle stabilisation.

Firstly, the component of the supporting torque that corresponds to the yaw angle was set to zero. The remaining components of the supporting force and torque were unchanged. Then the gait simulation was performed. Animation showed that after a few steps the biped turned about yaw axis and then fell over. It was not surprising, since the yaw angle was not controlled. The heuristic method proposed in this case consisted in introducing some changes into the torques that drive left and right hip joints (each hip joint consists of three consecutive revolute joints: α_1, α_2 and α_3). These changes were made in order to prevent the biped trunk from not controlled turning about the yaw axis. The functions defining torques in α_2 and α_3 joints were modified:

$$M_{\alpha_2} = \kappa\ (\alpha_{02} - \alpha_2 + \sin\alpha_1 \Delta_\xi) + \upsilon\ (\dot{\alpha}_{02} - \dot{\alpha}_2),$$

$$M_{\alpha_3} = \kappa\ (\alpha_{03} - \alpha_3 - \cos\alpha_1 \Delta_\xi) + \upsilon\ (\dot{\alpha}_{03} - \dot{\alpha}_3),$$

$$\Delta_\xi = \begin{cases} \delta\,(\theta_0 - \theta) & \text{during the support phase} \\ 0 & \text{during the swing phase} \end{cases}$$

where:

θ_0, θ - yaw angle given by the gait pattern and the current yaw angle, respectively

In the next few simulations of the biped gait the appropriate (i.e. leading to a stable gait) value of δ constant was chosen.

Similar procedures (the yaw angle stabilisation algorithm is one of the simplest) were used for the other components of the supporting force and torque. As a result a stable gait without the additional external supporting force and torque was achieved. The stable walking is a result of cooperation of several algorithms. The movement realised by the biped is slightly different from that given by the gait patterns. These differences are necessary for stabilisation of the gait. The utilised control algorithms are rather simple, nevertheless they enable the biped to walk.

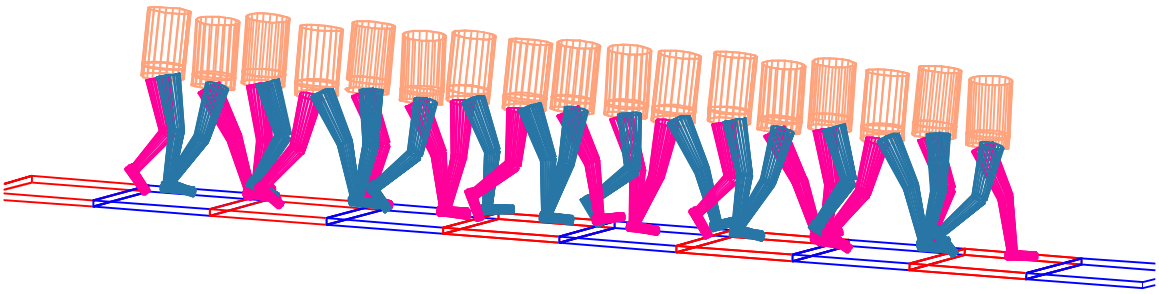

Figure 7. Superimposed frames from stable walk animation.

The control system of the biped is not engaged in planning of the trajectory, this task is realised following the gait patterns. The main task of the control system is to modify slightly and instantaneously the prescribed gait in order to prevent the biped from loosing stability.

4. Simulation results

The model is built in ADAMS 9.1 environment. During simulations Adams-Gear and DASSL integration procedures were utilised. The integration procedures parameters were changed to ensure that simulation results remained unchanged. The multibody model behaviour sensitivity to the control algorithm and the model parameters was checked. It was shown that positioning of the three-component force objects on the feet exerts the strongest influence on the model behaviour.

In the direct dynamics approach the ground reaction forces are computed (they do not play the role of input data). Comparison of the measured ground reaction forces with the calculated ones was used to validate the model. The comparison is illustrated in Fig. 8a. The calculated and the measured results are similar, however there are some differences. These differences are caused mostly by the fact that foot is modelled as one rigid body and a contact between foot and ground is reduced to five points only. To obtain better results the model of foot and the model of contact should be made more sophisticated. Approximations of measured walk parameters by periodical and symmetric gait patterns is another reason for differences - simulated ground reaction forces are much more regular, than measured ones. Simplifications made during the modelling process are also factors in obtained differences.

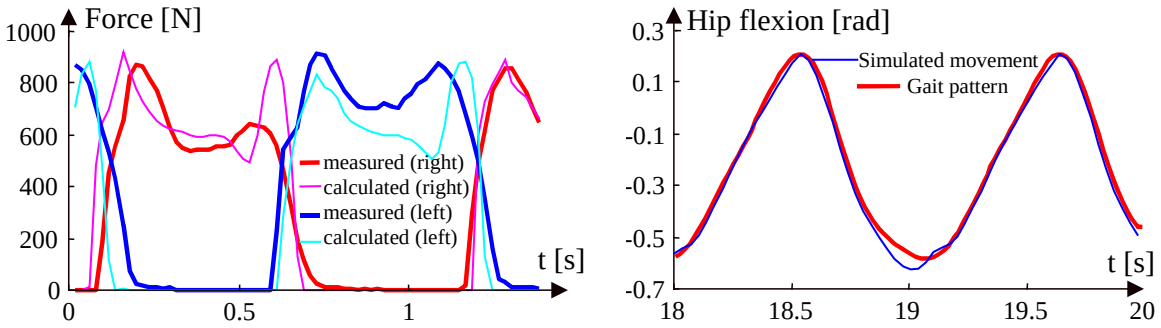

Figure 8. Calculated and measured results:
a) vertical ground reaction forces, b) right hip flexion angle.

The observed differences between measured and simulated data are less than 15% of maximal values, which is a decent result when biomechanical calculations are considered.

The control algorithms introduce some differences between the simulated motion and prescribed gait patterns (see Fig. 8b). These differences are relatively small, however big enough to maintain the biped stability.

5. Concluding remarks

ADAMS is a powerful tool, which enables using the direct dynamic approach to human gait analysis. Using this approach is possible to predict system behaviour. There is no need for ground reaction force measurements. Gait patterns can be extrapolated therefore the simulation

is not limited by the duration of measurements. The model was successfully validated. The results of simulation show reasonably good agreement with measurements.

6. References

ADAMS User's Kit. Mechanical Dynamic Inc., 1997.

Allard P., Stokes I. A. F., Blanchi J.-P. (ed.): *Three-Dimensional Analysis of Human Movement.* Human Kinetics Publishers, Champaign, Illinois, 1995.

Berme N., Cappozzo A. (ed.). *Biomechanics of Human Movement*. Ohio, USA, 1990.

Bourassa P., Prince F., Meier M., Roy Y.: *A simple walking model; simulation and animation.* Proc. of VIth International Symposium on Computer Simulation in Biomechanics, pp. 1 - 4, Tokyo, 1997.

Gerristen K. G. M., Van den Bogert A. J., Nigg B. M.: *Direct dynamics simulation of the impact phase in heel-toe running*. Journal of Biomechanics, Vol. 28, pp. 661 - 668, 1995.

Gilchrist L. A., Winter D. A.: *A two-part, viscoelastic foot model for use in gait simulations.* Journal of Biomechanics, Vol. 29, pp. 795 - 798, 1996.

Güler H. C., Berme N., Simon S. R.: *A viscoelastic sphere model for the representation of plantar soft tissue during simulations.* Journal of Biomechanics, Vol. 31, pp. 847 - 853, 1998.

Koopman B., Grootenboer H. J., de Jongh H.: *An inverse dynamics model for the analysis, reconstruction and prediction of bipedal walking*. Journal of Biomechanics, Vol. 28, pp. 1369 - 1376, 1995.

McCaw S. T., DeVita P.: *Errors in alignment of center of pressure and foot coordinates affect predicted lower extremity forces.* Journal of Biomechanics, Vol. 28, pp. 985 - 988, 1995.

Onyshko S., Winter D. A.: *A mathematical model for the dynamics of human locomotion*. Journal of Biomechanics, Vol. 13, pp. 361 - 368, 1980.

Ouezdou F. B., Bruneau O., Guinot J.-C.: *Dynamic analysis tool for legged robots*. Multibody System Dynamics, Vol. 2, No 1, pp. 369 - 391, 1998.

Pandy M. G., Berme N.: *Synthesis of human walking: a planar model for single support.* Journal of Biomechanics, Vol. 21, pp. 1053 - 1060, 1988.

Seireg A., Arvikar R.: *Biomechanical Analysis of the Musculoskeletal Structure for Medicine and Sport*. Hempshire Publishing Co, New York, 1989.

Van den Bogert A. J., Schamhardt H. C., Crowe A. *Simulation of quadrupedal locomotion using a rigid body model.* Journal of Biomechanics, Vol. 22, ss. 33 - 41, 1989.

Vaughan C. L., Davis B. L., O'Connor J.: *Dynamics of Human Gait.* Human Kinetics Publishers, Champaign, Illinois, 1992.

Vint P. F., Hinrichs R. N.: *Endpoint error in smoothing and differentiating raw kinematic data: an evaluation of four popular methods*. Journal of Biomechanics, Vol. 29, pp. 1637 - 1642, 1996.

Winter D. A. *Biomechanics of Human Movement*. John Wiley & Sons Inc., 1979.

Wojtyra M.: *Applicability of human gait patterns to biped gait control - computer simulation.* Proc. of the 12th CISM-IFToMM Symposium on Theory and Practice of Robots and Manipulators, pp. 393 - 400, CISM, Udine, 1998.

Wojtyra M.: *Dynamical simulation of human walking*. Proc. of Tenth World Congress on the Theory of Machines and Mechanisms, pp. 1853 - 1858, Oulu, Finland, 1999.

DYNAMICAL ANALYSIS OF HUMAN WALKING

Marek Wojtyra

Institute of Aeronautics and Applied Mechanics
Warsaw University of Technology

Presentation topics

- Introduction - reasons for gait analysis
- Multibody model
  - » Kinematical and mass properties
  - » Ground reaction forces
- Control system
  - » Gait patterns
  - » Driving forces
  - » Control algorithms
- Simulation results

Reasons for performing gait analysis

Collecting information about:

- muscle forces and bone loads
- energy consumption
- control strategies

Applications in:

- medicine
- ergonomics
- sport
- technology (walking machines)

Multibody model

Kinematical and mass properties

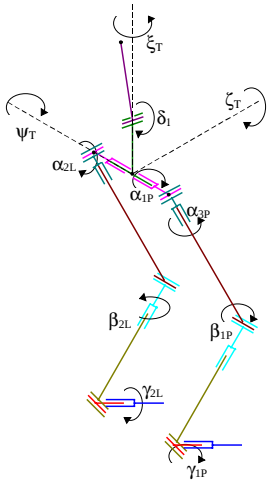

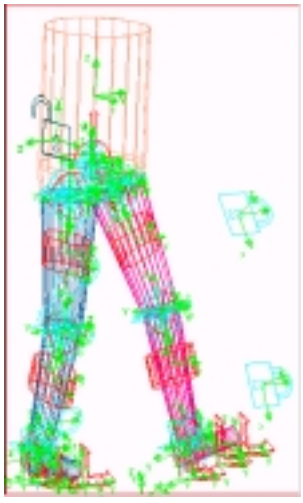

Multibody model

Ground reaction forces

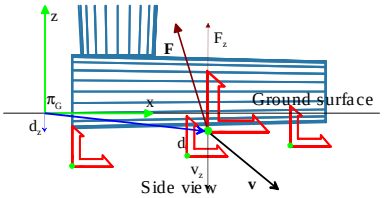

$$F_z = \begin{cases} MAX(0\ ,\ -k\,d_z - c\,v_z) & d_z < 0 \\ 0 & d_z \geq 0 \end{cases}$$

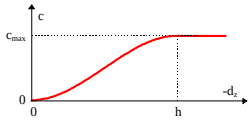

$$v = \sqrt{v_x^{\,2} + v_y^{\,2}}$$

$$\mu' = \mu\,\frac{2}{\pi}\,\mathrm{arctg}\,\frac{v}{\lambda}$$

$$T = \mu'\,F_z$$

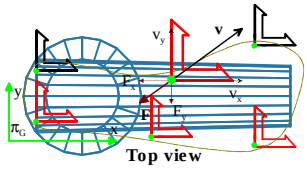

Top view

$$F_x = -T\,\frac{v_x}{v+\varepsilon} \qquad F_y = -T\,\frac{v_y}{v+\varepsilon}$$

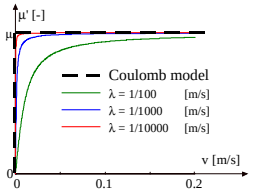

Control system

Gait patterns calculations

Measured trajectories of selected points

Geometrical calculations

Relative angles in joints

Subject session

Periodization

Symmetrization

Gait patterns

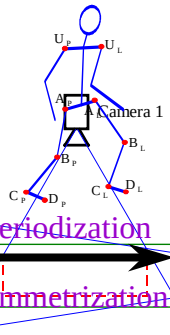

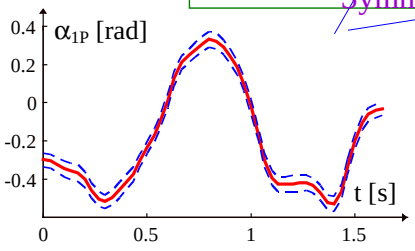

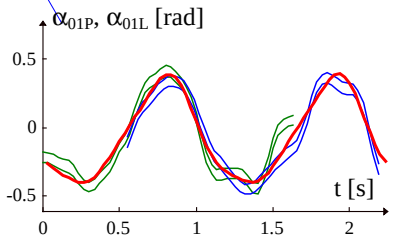

Control system

Driving torques

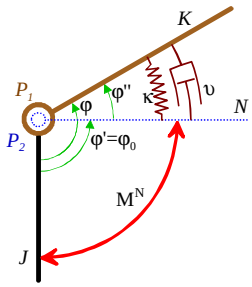

Driving torque in i-th joint:

$$M_i^N = \kappa_i(\varphi_{0i} - \varphi_i) + \upsilon_i(\dot{\varphi}_{0i} - \dot{\varphi}_i)$$

desired ang
(gait patter

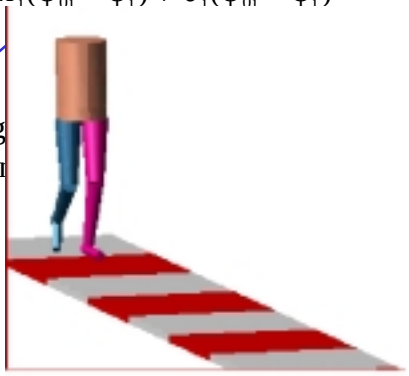

Control system

Control algorithms

Example: trunk yaw angle control

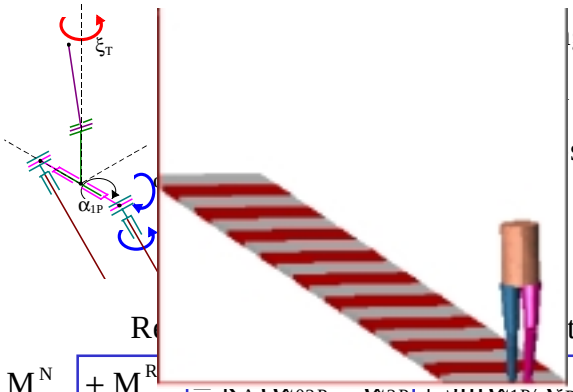

g torques:

$\alpha_{1P}\Delta_{\xi P}$

s$\alpha_{1P}\Delta_{\xi P}$

stance phase

swing phase

R ts:

$$M_{\alpha_{2P}} = M^N_{\alpha_{2P}} + M^R_{\alpha_{2P}} = \kappa_A(\alpha_{02P} - \alpha_{2P} + \sin\alpha_{1P}\Delta_{\xi P}) + \upsilon_A(\dot{\alpha}_{02P} - \dot{\alpha}_{2P})$$

$$M_{\alpha_{3P}} = M^N_{\alpha_{3P}} + M^{R_\xi}_{\alpha_{3P}} = \kappa_A(\alpha_{03P} - \alpha_{3P} - \cos\alpha_{1P}\Delta_{\xi P}) + \upsilon_A(\dot{\alpha}_{03P} - \dot{\alpha}_{3P})$$

Simulation results

Checking the sensitivity to changes of:

- integration procedures parameters
- dimensions and masses
- contact parameters
- control algorithms parameters
- driving torques parameters

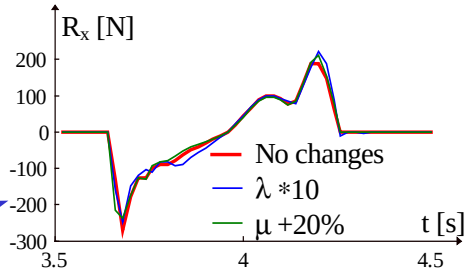

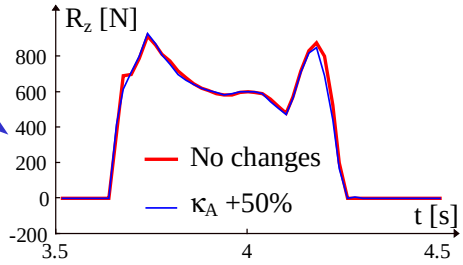

Simulation results

Simulated movement vs. gait pattern

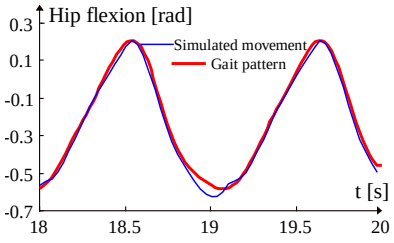

Simulated ground reactions vs. measured ground rreactions

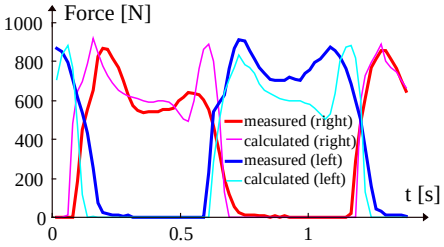

Concluding remarks

•ADAMS is a powerful tool, which enables using the direct dynamic approach to human gait analysis.

•Using this approach is possible to predict system behaviour.

•There is no need for ground reaction force measurements.

•Gait patterns can be extrapolated therefore the simulation is not limited by the duration of measurements.

•The model was successfully validated. The results of simulation show reasonably good agreement with measurements

Thank you very much